INDONESIAN JOURNAL ON GEOSCIENCE
Geological Agency
Ministry of Energy and Mineral Resources

Journal homepage: http://ijog.geologi.esdm.go.id
ISSN 2355-9314, e-ISSN 2355-9306

The Use of Electrical Resistivity Tomography and Time Domain Electromagnetic Methods to Investigate the Superficial Deposits at Al al-Bayt University, Jordan as a Case Study

Fatima Ghanem, Hani Al Amoush, and Eid Al-Tarazi

Earth and Environmental Department, Al al-Bayt University, Mafraq, Jordan
Department of Earth and Environmental Sciences, Prince El Hasan Bin Talal Faculty of the Natural Resources and Environment, The Hashemite University, Jordan

Corresponding author: hani.alamoush1@gmail.com
Manuscript received: June, 1, 2020; revised: August, 21, 2021;
approved: May, 14, 2022; available online: October, 7, 2022

Abstract - In this study, an integration of Electrical Resistivity Tomography (ERT) and Time-Domain Electromagnetic (TDEM) methods have been used to investigate the superficial deposit characterization at Al al-Bayt University area. ERT and TDEM results helped to delineate the subsurface geology, and to map soil and basalt flow thicknesses as well as subsurface geological structures. Superficial deposit thicknesses were found in the range of 9 to 16 m, whereas the underlying basalt flow thickness was found to vary from a few meters in the western part to more than 60 m in the most eastern part of the studied area. The ERT results permitted a subsurface lithology characterization of the upper 35 m below ground surface (mbgs), the soil/superficial deposit resistivity was found in the range of 5–40 Ohm.m, and thickness within 12–15 mbgs. The TDEM results permitted mapping and delineating the subsurface geology up to 80 m, and allowed mapping the main subsurface structures. The soil/superficial deposits have resistivity in the range of 10 to 90 Ohm.m and the thickness in the range of a few meters up to 15 m. The study recommends a detailed geophysical study before starting any type of geo-engineering construction.

Keywords: ERT, TDEM, superficial deposits, Al al-Bayt University, Jordan

How to cite this article:
Ghanem, F. and Al Amoush, H. 2022. The Use of Electrical Resistivity Tomography and Time Domain Electromagnetic Methods to Investigate the Superficial Deposits at Al al-Bayt University, Jordan as a Case Study. *Indonesian Journal on Geoscience*, 9 (3), p.355-369. DOI: 10.17014/ijog.9.3.355-369

Introduction

Background

The Al al-Bayt University has a large surface area that is continuously under construction and expansion. It is essential to study the properties and structures of the soil foundation, to delineate the depth to bedrock, and to map the spatial variations of soil thickness to support urban and constructional expansion plans of the university buildings by using geophysical methods.

Traditional and modern geophysical techniques have presently been very common and considered as an effective tool to explore the subsurface features for different applications. For instance, geotechnical engineering, environmental groundwater aquifer characterization (Nugraha *et al*. 2021), mineral explorations, and geomorphology that include sediment thickness. Geophysical exploration methods have acquired great importance, because they are nondestructive and reliable, and are often less expensive

compared to other methods such as drillings, fast field application, and high resolution data collection in short time (Otto and Sass, 2006; Al-Amoush and Mashagbeh, 2009; (Farid *et al*. 2021).

The Electrical Resistivity Tomography (ERT) technique is used in shallow applications around tens of meters, while the Time Domain Electromagnetic method (TDEM) technique is used for deep applications around hundreds of meters, and it can detect layers of different conductivities (McNeill,1994; Christiansen *et al*., 2006; Rangel *et al*., 2018). The ERT method is considered as a strong tool to study subsurface geological features for different engineering, geotechnical, and environmental applications (Al Amoush and Abu Rajab, 2018; Olasunkanmi *et al*., 2021). In addition, it could characterize sediment deposits and map recent deposits, as well as map the depth to bedrock. It can be used to map the thickness of the sediment covering bedrock (Hsu *et al*., 2010; Sauret *et al*., 2015; Al-Amoush *et al*., 2017). The TDEM method measures the difference of electrical conductivity in the subsurface. It has widely been used in hydrogeological exploration and geological mapping applications such as mapping sand, gravel, clayey layers, and depth of bedrock (Al Amoush *et al*., 2016). There is a strong relationship between electrical conductivity and soil properties. TDEM techniques are useful tools for soil mapping at different depths (Danielsen *et al*., 2003; Thomsen *et al*., 2004; Bauer-Gottwein *et al*., 2010; French, 2011).

Studying soil characteristics, soil thickness, and elastic properties of soil in different parts of the world have been the focus of multiple geophysical studies. For instance, Diallo *et al*. (2019) used Electrical Resistivity Tomography (ERT) method in Canada in order to characterize the subsurface stratigraphy, mapping bedrock topography, and determine overburden thickness. Al-Heety and Shanshal (2016) used ERT and Seismic Refraction Tomography (SRT) to study subsurface strata in Mosul University, Iraq, to produce subsurface geological feature maps and soil property maps. Ghanem *et al*. (2021) used multi-analysis shear wave (MASW) and seismic refraction tomography (SRT) to investigate superficial deposits at Al al-Bayt University, Jordan. Porsani *et al*. (2012) used the TDEM method and borehole data in Brazil, to a geoelectrical mapping of sedimentary, basalt layers, and geological fractures.

In this study, an integration of geophysical methods composed of Electrical Resistivity Tomography (ERT) and Time-Domain Electromagnetic (TDEM) methods have been conducted, to investigate the superficial deposits and soil characterization in Al-al Bayt University and its surrounding areas. ERT and TDEM methods were used to delineate the subsurface geology and to map soil and basalt flow thicknesses as well as the subsurface geological structures.

Researched Area

Al al-Bayt University covers an area of about 7.539 x 10^6 m^2 (https://www.aabu.edu.jo). It lies between 238826 to 243626 E and 3582320 to 3578820 N according to Universal Transverse Mercator (UTM) coordinate system (Figure 1). It is located in Mafraq Governorate, northeast Jordan. Jordan with a surface area of 89.400 km^2, is characterized by a Mediterranean climate and considered as an arid to semi-arid region. The annual precipitation is 300 mm, rainfall is erratic in both spatially and temporarily (Al-Kloub and Al-Shemmeri, 1995; Jaradat *et al*., 1999; Baban and Al-Ansari, 2001; Qdais and Batayneh, 2002; Afonso *et al*., 2004; Al-Momani, 2008; Abdulla and Al-Shareef, 2009; Ministry of Water and Irrigation (MWI), 2016). Figure 2 shows the geological map of the studied area. The studied area is composed of superficial deposits (Quaternary age), and consists mainly of two soil types: the red soil and the desert soil (Smadi, 1997; Gharaibeh, 2003).

Methodology

The adopted methodology used in this study is illustrated in the flowchart shown in Figure 3.

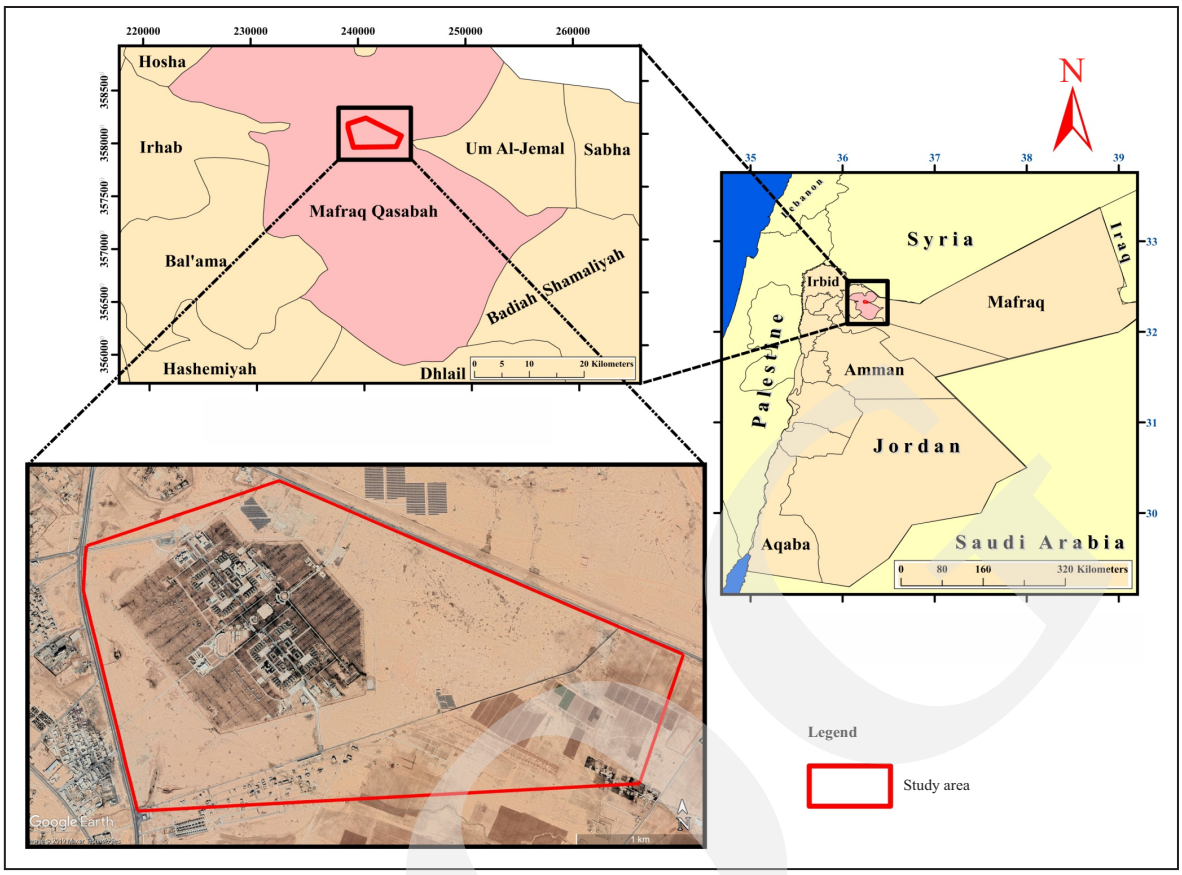

Figure 1. Location map of the studied area (Al al-Bayt University and its surrounding areas).

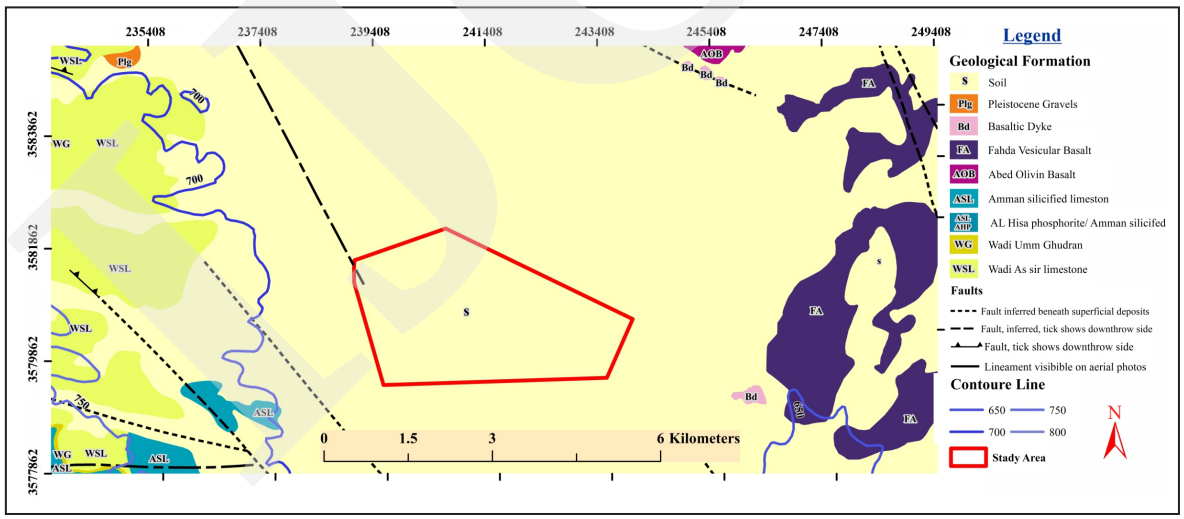

Figure 2. Simplified geological map of the studied area (Modified after Smadi, 1997; Gharaibeh, 2003).

Subsurface Geological Mapping

To review and to understand the surface and subsurface geological setting of the studied area, the following data resources have been collected, reviewed, and investigated, *i.e.* surface geological map of the studied area (Smadi, 1997; Gharaibeh, 2003) and groundwater well logs inside and outside Al al-Bayt University area (MWI, 2018) and available geoengineering borehole logs.

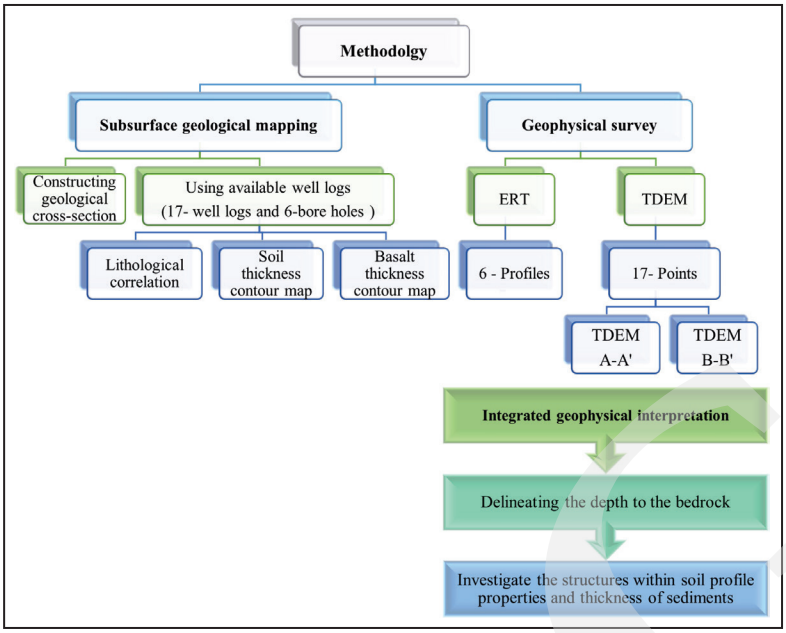

Figure 3. Flow chart displays the adopted methodology used in this research.

Geophysical Survey

Electrical Resistivity Tomography

The direct current (DC) or very low frequency resistivity technique is used to measure the subsurface resistivity (ρ). This method is widely used because of its relatively easy principle and interpretation. The fundamental principle of the method is relying on injecting an electrical current into the subsurface by a pair of current electrodes (C1 and C2) and measuring the potential difference (ΔV) between another two pairs of potential electrodes (P1 and P2). The current electrodes (C1, C2) act as a source and sink, respectively (Lowrie, 2007).

The ground apparent resistivity (ρ_a) is given as:

$$\rho_a = 2\pi \frac{v}{1}\left\{\frac{1}{C1P1}-\frac{1}{P1C2}-\frac{1}{C1P2}+\frac{1}{P2C2}\right\}^{-1} \quad \text{..... (1)}$$

where:
1 is the electric current measured in Ampere,
(v) is voltage.

The calculated apparent resistivity depends on *injected current (I), the voltage (v) measured, and the geometrical factor (K)* (Reynolds, 1997). Apparent resistivity measurements are then *inverted to produce models of the subsurface geology based on its electrical properties* (deGroot-Hedlin *et al*., 1990; Wolfe *et al*., 2000). *The inverted models can be used to delineate and to identify the subsurface features such as bedrock depth, fracture zones, conductive, resistive zones, and lithological units* (Benson *et al*., 1997; Dawson *et al*., 2002).

Data Acquisition and Processing

In the present study, six 2-D ERT profiles have been used (Figure 4). The 2-D electrical resistivity tomography surveys were performed with lengths of 240 m, using a multichannel system contained 48-electrode. The spacing between every two adjacent electrodes was 5 m. The multi-channel system automatically operates once to identify the type of electrical con-figuration and geometrical parameters.

The SYSCAL Junior Switch (IRIS Instruments) resistivity meter was used for resistivity measurements. The Dipole-Dipole electrical electrode configuration was selected. This configuration is characterized by its high resolution for detecting vertical and horizontal variations (Loke, 2014). The device is controlled by an internal microprocessor together with a

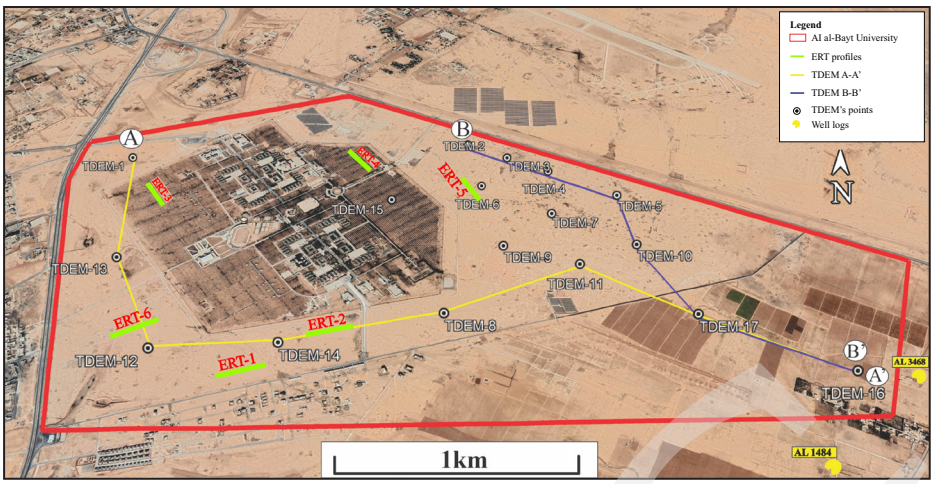

Figure 4. Location map of geophysical measurement ERT, TDEM, and TDEM cross-sections.

switching unit for automatic to record hundreds of resistivity measurements independently (Loke, 2014). Electrical resistivity tomography (ERT) is commonly used using twenty-four electrodes or more, attached to multicore cable (Griffiths and Barker, 1993; Reynolds, 2011).

Resistivity measurements are recorded and saved in the SYSCAL resistivity meter device automatically after instrumentation and field setup. The sequence of measurements, for example, electric current duration, survey parameter, and type of configuration can be set manually in the field or preliminary prepared, and uploaded to the laptop microprocessor system (Al-Amoush *et al*., 2017).

ELECTRE PRO (V02.03) software (Iris instruments, 2007) was utilized to produce the measurement sequence. PROSYS II (V03.07.05) was used to access, to edit, and to filter the stored data after completion of the field survey, and RES2DINV version, 3.71 (Loke, 2014) modeling software was used to produce inverted resistivity models for measured data. The topography change in the investigated sites is very small, so the topographical corrections was not applied to resistivity measurements.

Time Domain Electromagnetic (TDEM)

A model of TDEM array is made up of a transmitter loop and a receiver coil, generating a very strong current (from 1 to 20 Ampere) by battery or by a motor-generator, and injecting current into a square loop (commonly single turn) by a wire put on the surface and immediately linked to the transmitter. The transmitter current is a modified symmetrical square wave (Ranieri, 2000).

After each second quarter-duration, the transmitter current is abruptly decreased to zero for the one-quarter duration, thus it flows in the reverse trend. A voltage pulse is recorded in a receiver loop during the current is switched off. The receiver loop can be coincident or inside the transmitter loop. The required depth of the study equal to about the side length of the loop. The loop aspect varies from a few meters to hundreds of meters. According to Faraday law, when the process of sudden decreasing transmitter current to zero induces a small period voltage pulse in the subsurface, this leads to the loop of current to flow in the direct proximity of the transmitter wire (Ranieri, 2000).

Directly after the transmitter direct current has been turned off, the current loop passes into the subsurface directly below the transmitter and on account of finite resistivity of the subsurface, the current amplitude begins to decay. In the same way, the decaying current produces a voltage pulse, which allows more current to flow at a greater distance from the transmitter loop and therefore at a greater depth (McNeill, 1994). The decaying signals measured at several delay

times are then transformed into one-dimensional resistivity of the ground (McNeill, 1990; Nabighian and Macnae, 1991).

To determine the voltage generated by the decaying magnetic field at the receiver coil at successively later times, measurements are made of the current flow and of the electrical resistivity of the subsurface at increasingly depths, and it is this process that forms the foundation of resistivity (McNeill, 1994).

TEM-FAST 48HPC instrument (Advanced Electromagnetic Research (AEMR) (AEMR, 2013) is a very effective tool to study shallow subsoil and hydrologic electromagnetic properties by measuring them through a short time after the transmitter current is switched off (Ranieri, 2000).

Data Acquisition And Processing

Seventeen TDEM sounding points were conducted in the studied area (Figure 4). TEM-FAST 48HPC instrument system (AEMR, 2013) which includes a transmitter-receiver controller and managed by the HP-IPAQ pocket system was used for data collection. A single turn of 50 m × 50 m loop was used to get a sufficient penetration depth around one hundred meters. The system used twelve voltage batteries with forty-eight active time gates (15,360 μs - t centre) to produce an electrical current up to 4 Ampere, and the system was set up for a 50 Hz notch filter. The measurement recording time was set for seven minutes which achieved a maximum transient delay time of one millisecond.

TEM sounding data were processed to provide 1-D resistivity model with depth. Several processing steps were conducted before inversion and included editing, smoothing, and accounting for induced polarization (IP) and Supermagnetism (SPM) (Barsukov *et al*., 2007). The 1-D and 2-D apparent resistivity cross sections were obtained by a transformation procedure provided by TEM-RES Software (AEMR, 2015) based on the normalized voltages ($E(t)$ / I) (Barsukov *et al*., 2007).

The building of apparent resistivity cross section $\rho(t)$ can be done using transformation procedure. The trans-formation follows the direct procedure of Barsukov *et al*. (2007:

$$E(t) / I \rightarrow \rho(t) \rightarrow \rho(h) \quad \text{..... (3)}$$

Based on the quality of the TEM data, they were subjected to filtering procedure and noise cut off before modeling and inversion steps. The data were examined for the SPM and IP effects. The sites of TEM measurements were selected to be far from any type of electromagnetic noise such as electric power lines or any artificial objects and constructions. The transient response shows a high signal to noise (S/N) ratio.

In general, the 1-D modeling result provides a reasonable representation of the true resistivity model. A 3-D effects can influence the 1-D model in the case of a lateral geological contrast is overcome. The root mean square (rms) of the final data misfit was < 5%. This is an indication that the obtained TEM measurements are of high quality. The root mean square (rms) for ERT was less than 15.4%. Different 2-D pseudo- and inverse resistivity sections from 1-D sounding resistivity were obtained, and helped in interpreting reliable TDEM measurements and defining the subsurface geological structures. The ERT survey is designed so that it is possible to record 785 point measurement (quadri-poles) arranged over twenty-five levels below earth surface, and with apparent investigation depth of 32 m.

Results and Discussions

Subsurface Geological Cross Sections

Figure (5) shows the surface geological map of the studied area, and an E-W geological cross-section crossing the studied area has been constructed. Two lithological correlation sections between the groundwater well logs in the studied area have been performed (Figure 6). In cross section 1, the superficial/soil deposit layer was found in all groundwater well logs except well AL1484 and well AL3082 (Figure 7). The superficial deposit thickness increases in the

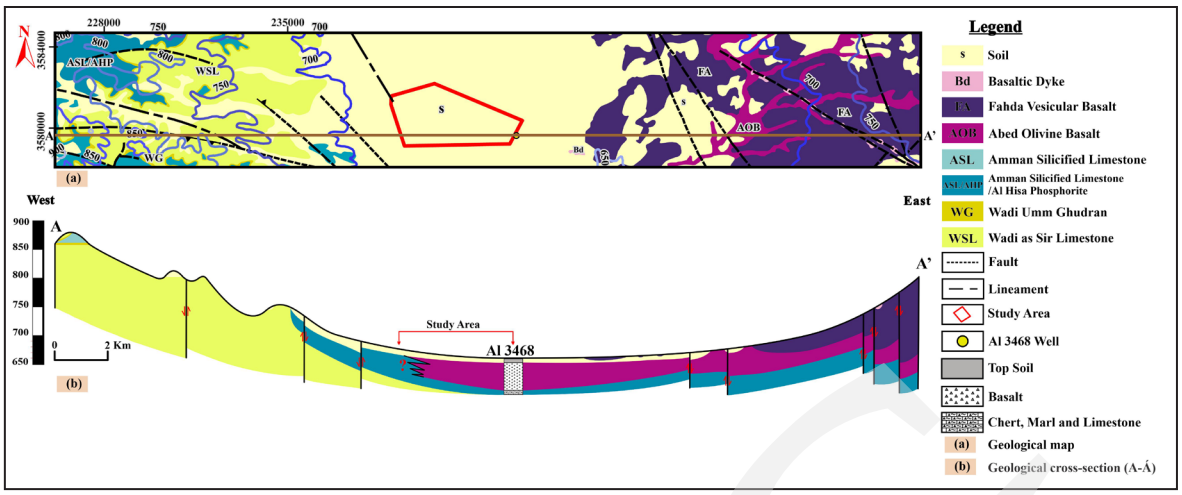

Figure 5. a. Simplified geological map of the studied site and its surrounding areas (Smadi, 1997; Gharaibeh, 2003); b. Geological cross-section (A-Á) deduced from the geological map, correlated with (Al 3468) well log (Ministry of Water and Irrigation (MWI, 2018).

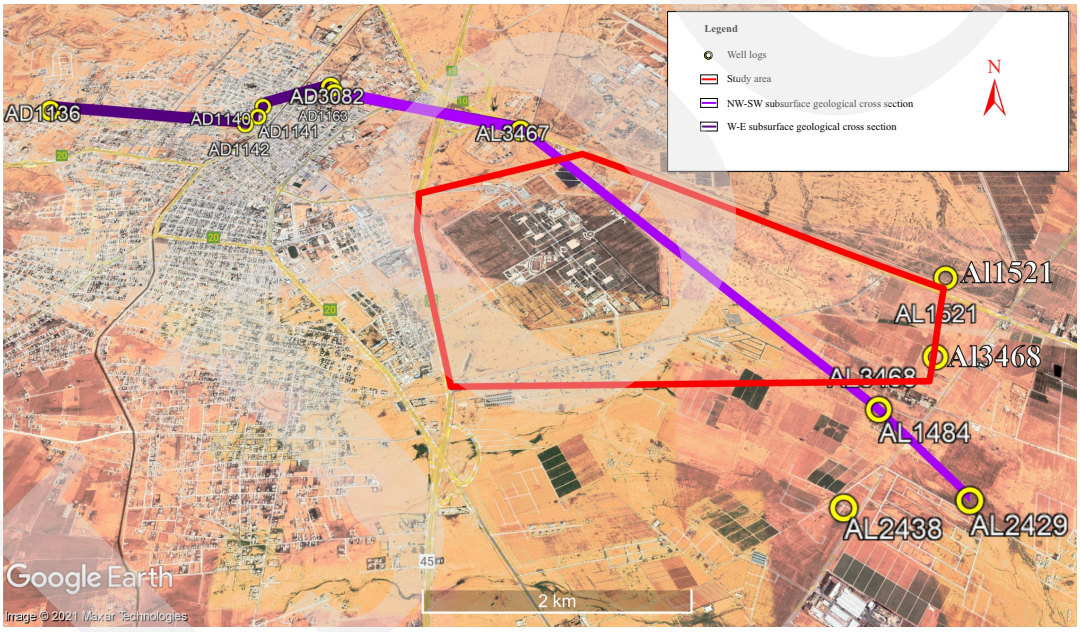

Figure 6. Lithological cross section locations and extensions.

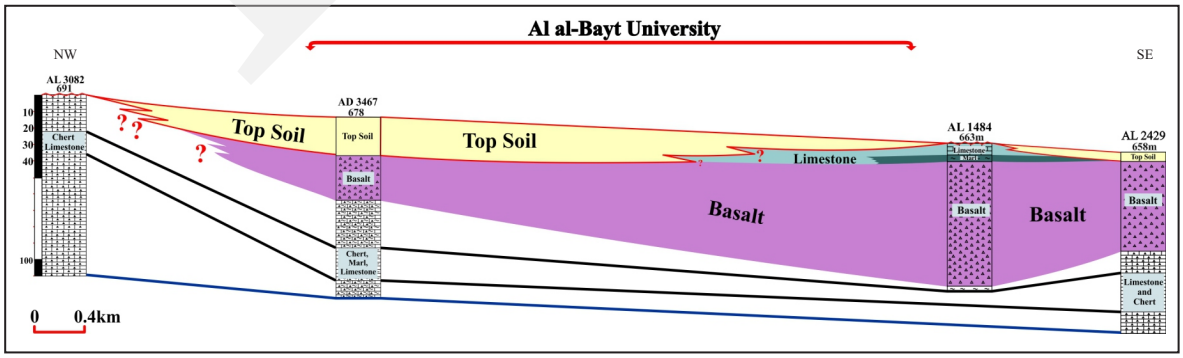

Figure 7. NW-SW subsurface geological cross section between groundwater well logs across the studied area.

middle of the section, and reaches to about 20 m decreasing into SE direction. Basalt flow layer was found along the cross section-1 (Figure 7). Its thickness was found to be in the range of 25 m in AL3467 to 75 m in AL1484 log. Figure 8 shows a lithological correlation of the groundwater well logs in the western part of the studied area. The results show the superficial deposit layer exists in all well logs, except AD1136, AD1142, and AL3082 wells. While there is no basalt flow layer across this section.

Soil and Basalt Flow Thickness *Contour Maps*

The thickness of topsoil layer deposit and basalt flow layers in each groundwater well logs in the studied area has been extracted, and a contour map for top soil and basalt layers were created using Kriging interpolation method within ArcGIS10.3 environment.

The results are presented in Figures 9a and 9b, respectively. The soil thickness is ranging from a few meters in the most western and southwestern parts of the studied area to more than 15 m in NNW part of the studied area (Figure 9a). As for the basaltic flow layer (Figure 9b), the thickness of basaltic flow layer ranges from a few meters in the most western parts of the studied area to more than 60 m in the most eastern part.

Electrical Resistivity Tomography *(ERT) Interpretation*

Figure 10 shows the results of 2-D resistivity models correlated with available borehole logs in the studied area. The soil/bedrock boundary as deduced from soil thickness map of the studied area (Figure 9a) was correlated and overlaid the different ERT tomograms, and found to be

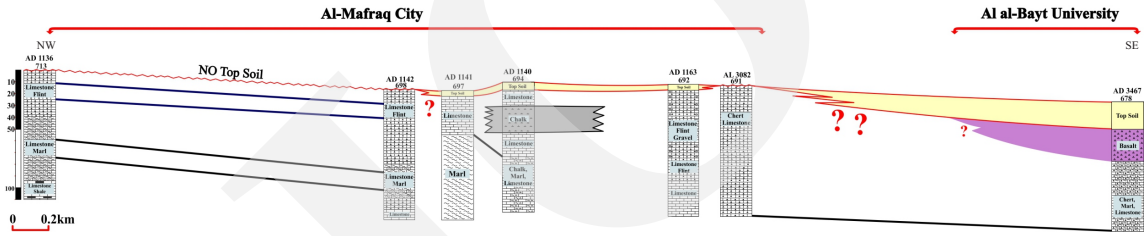

Figure 8. W-E subsurface geological cross section between well logs, west of the studied area. No superficial deposits (soil profile) were in the most western parts of the cross section, and it increases in an easterly direction.

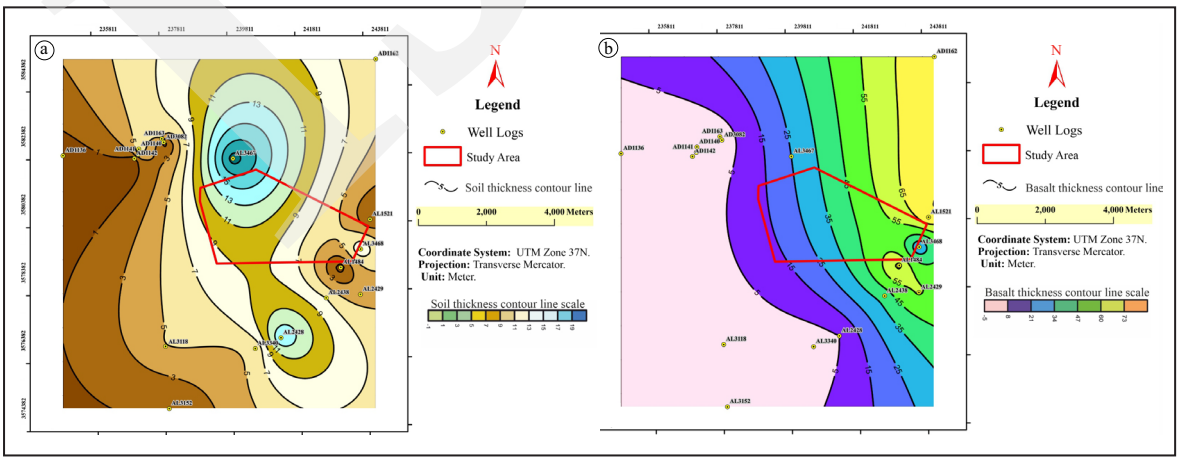

Figure 9a. Thickness of the soil superficial deposits in the studied area. 9b.Thickness of basalt flow layer in the studied area. The data used for creating these maps were deduced from the geological well logs in the studied area and interpolated using Kriging interpolation method in ArcGIS10.3 environment.

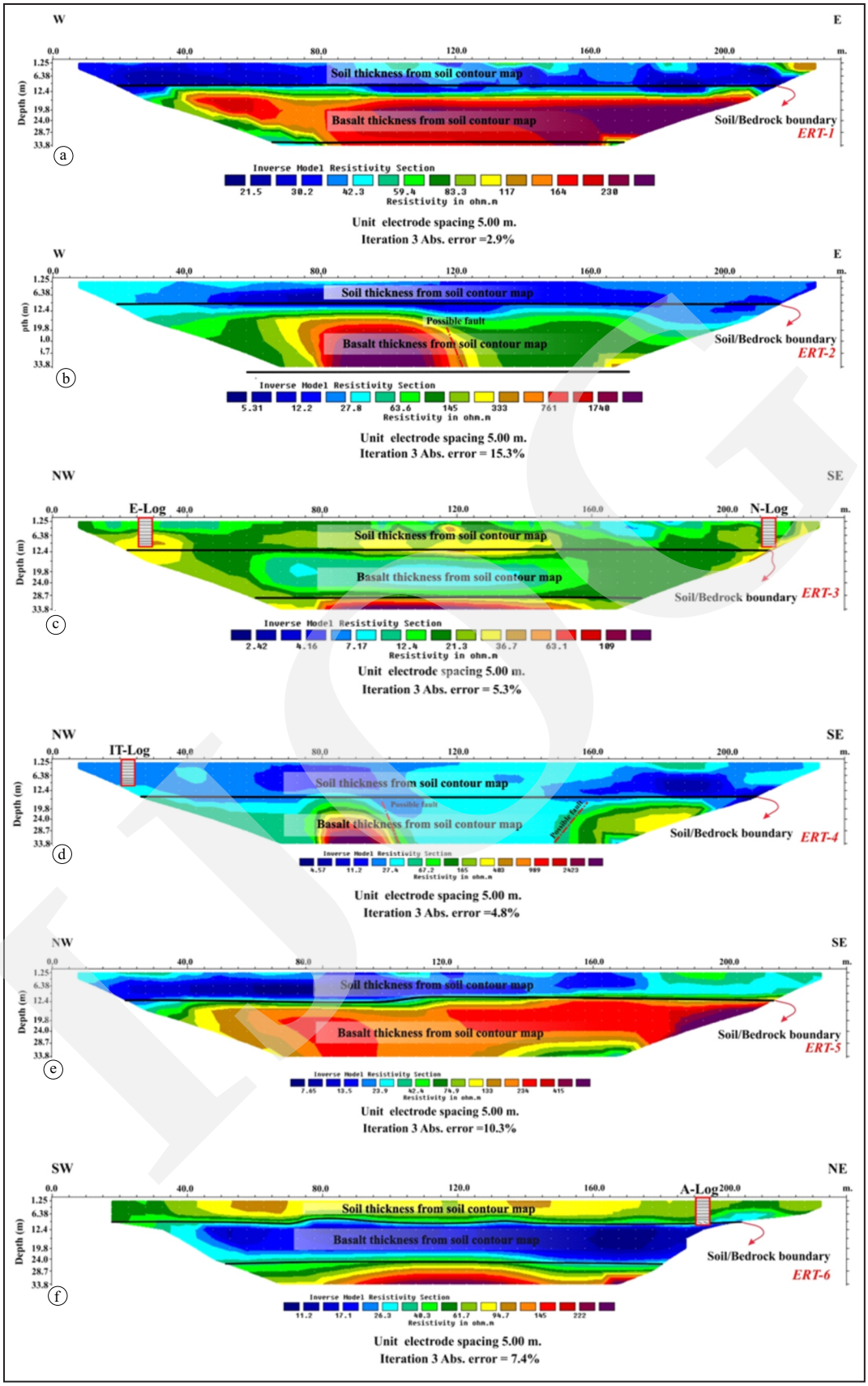

Figure 10. 2-D resistivity model tomograms with interpretation, calibrated with borehole logs in the studied area (a. ERT-1, b. ERT-2, c. ERT-3, d. ERT-4, e. ERT-5, and f. ERT-6).

highly correlated with the base of low resistivity layer (Figures 10a-f). The base boundary of basalt layer deduced from the basalt contour map (Figure 9b) was also well correlated with ERT tomograms (Figure 10). The results show a good correlation in ERT-3 and ERT-6 tomograms as indicated by distinctive resistivity contrast (Figures 10c and 10f). Two principle geoelectric resistivity layers were identified in the surveyed area. The first top layer consists of superficial deposits layer that has resistivity in the range of 5-90 Ohm.m, with the thickness of 12-15 m, found in all resistivity models (Figure 10). The second layer is correlated well with weathered basaltic layer. It has resistivities in the range of 150-1500 Ohm.m and the thickness of 17-22 m as shown in ERT-1, ERT-2, and ERT-5 (Figures 10a, 10b, and 10e, respectively). This layer characterized by low resistivity values (7 -30 Ohm.m) and thickness of 18-20 m in ERT-3, ERT-4, and ERT-6 tomograms (Figures 10c, 10d, and 10f, respectively). The low resistivity values for the second layer was attributed to the effect of water infiltration from irrigation activities in these locations. Moreover, the second subsurface layer has large lateral variations of resistivity (60 -1800 Ohm.m) (Figures 10b and 10d), and this is properly due to the lithological variations and/or due to a potential fault structure.

Time-Domain Electromagnetic (TDEM) *Interpretation*

Seventeen TDEM sounding points have been conducted in the studied area (Figure 4). The sounding TDEM-16 was conducted adjacent to AL3468 well which is located at a 310 m to the NW away of TDEM-16 for calibration purposes (Figure 11). The results show a good correlation between the boundaries of lithological units shown in the well log and the geoelectric layer boundaries as indicated by 1-D TDEM model. The results indicate that the topsoil layer is characterized by low resistivity values. The limestone and chert layers show an intermediate resistivity of around 100 Ohm.m. The basaltic flow layer shows high resistivity values (100 to >1000 Ohm.m). While, the most bottom marl layer was correlated with intermediate resistivity values. Consequently, this litho-resistivity relationship was used as a guide for interpretation the other 1-D and 2-D modeling results done in this study. The RMS error was in the range of 1-3.3 %. Figures 12 and 13 show 2-D geoelectromagnetic sections (TDEM-1 and TDEM-2). The TDEM sections were calibrated with the adjacent groundwater well log. The 2-D modeling results show that the resistivity is ranging from about 10 Ohm.m to higher than 2000 Ohm.m. The soil thickness across the cross sections has been picked from the soil contour map (Figure 9a) and overlaid on the TDEM sections. The topsoil layer is characterized by low resistivity values (10 - 70 Ohm.m) and the soil thickness ranges from a few meters to about 12 m in TDEM-1 (Figure 12). In TDEM-2 (Figure 13), the topsoil layer is characterized by low resistivity values (10−90) Ohm.m, and the thickness is ranging from a few meters to about 15 m in TDEM-2. The sections also show several potential geological structural features (faults) as indicated by large lateral variations in resistivity values.

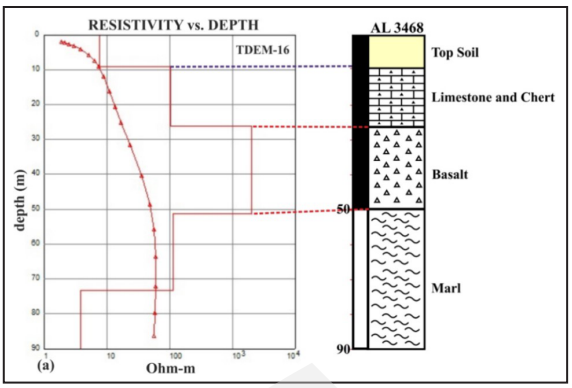

Figure11. Correlation and comparison of AL3468 well log with inverted TDEM-16 model.

Integrated Geophysical Interpretation

The obtained 2-D TDEM and 2-D ERT models were integrated for better understanding and characterizing the superficial deposits and subsurface geology in the studied area. Figure

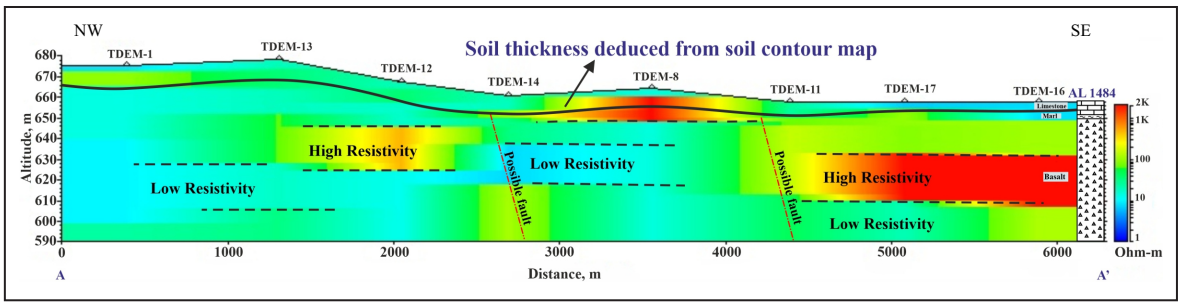

Figure 12. 2-D TDEM -A-A' correlated with AL3468 well log located at 0.31 km east of TDEM-16. See Figure 4 for TDEM sections locations.

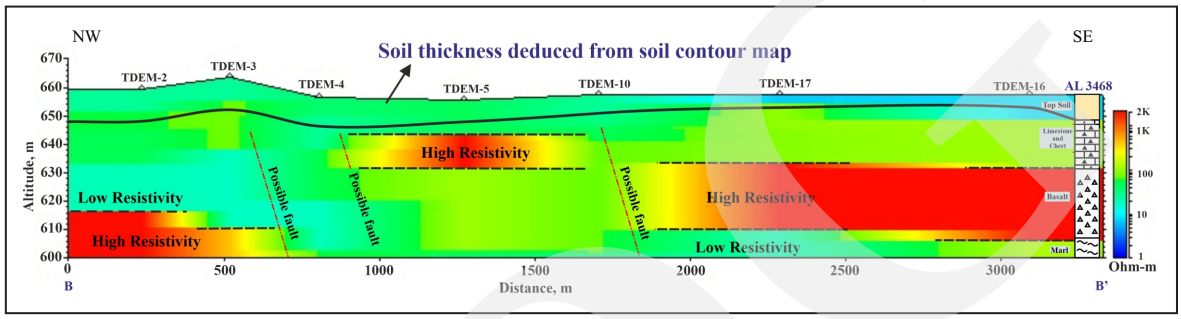

Figure 13. 2-D TDEM –B-B' correlated with AL3468 well log located at 0.31 km east of TDEM-16. See Figure 4 for TDEM sections locations.

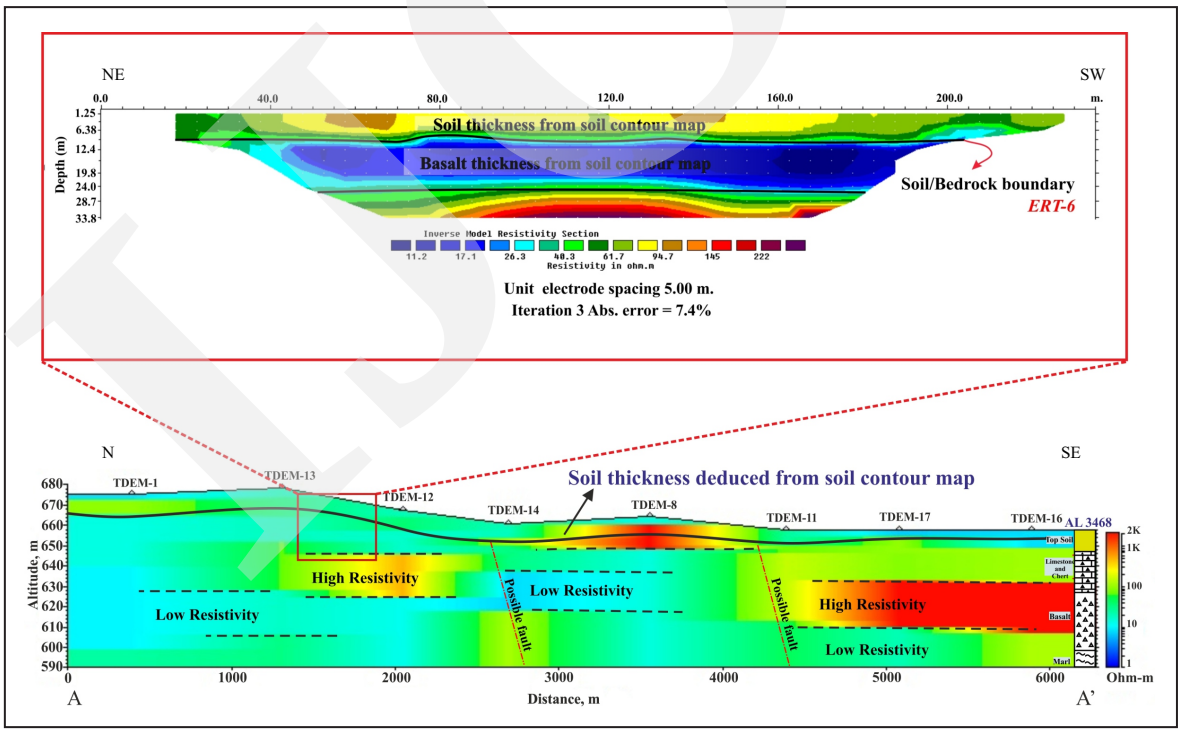

Figure 14. An integration between the TDEM-AA' model and ERT-6 model.

14 shows the interpreted TDEM-AA' model and interpreted ERT-6 model. ERT-6 model is located between TDEM-13 and TDEM-12. Figure 15 shows the interpreted TDEM-BB' model and the

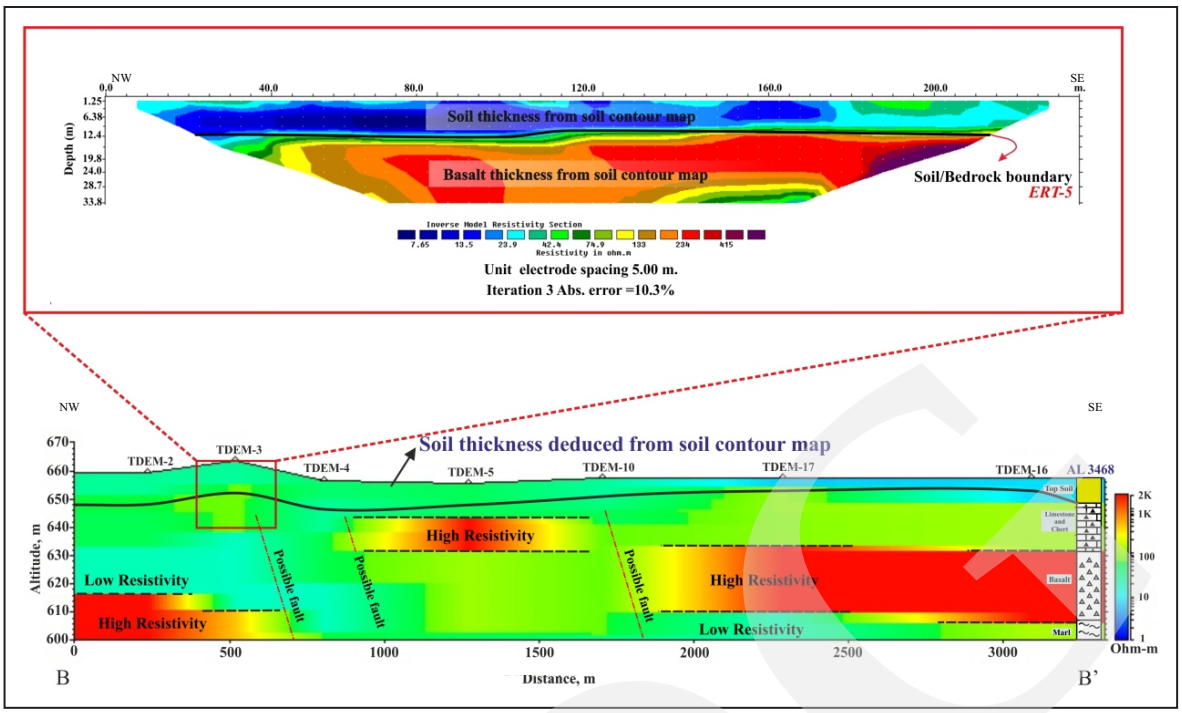

Figure 15. An integration between the TDEM-BB' model and ERT-5 model (150 m apart).

interpreted ERT-5 model. ERT-5 model is located between TDEM-2, TDEM-3, and TDEM-4. The ERT model is shown in the red rectangle. The integration shows a good correlation between the results deduced by both geophysical methods, especially the subsurface superficial deposits characterization, layering boundaries, and resistivity distribution.

Conclusions

In this study, an integration of two geophysical techniques composed of Electrical Resistivity Tomography (ERT) and Time-Domain Electromagnetic (TDEM) was performed. The integration between ERT and TDEM geophysical techniques was proved to be an efficient mean for near surface and superficial soil deposit characterization.

Electrical Resistivity Tomography (ERT) results permitted a subsurface characterization with a better resolution over TDEM results of the upper 35 m below ground surface. The soil/superficial deposit resistivity was found in the range of 5−40 Ohm.m), and the thickness within 12−15 m below the ground surface. A high correlation was found between the results of ERT's and soil thicknesses deduced from geological log data. The results of ERT also permitted mapping the subsurface layering/ boundaries and inferring some geological lateral variations and/or potential fault structures.

Time-Domain Electromagnetic (TDEM) results permitted mapping and delineating the subsurface geology up to 80 m below the ground surface. It also allowed mapping the main subsurface structures in the area under study. The TDEM results indicate that the soil/superficial deposits have resistivity in the range of 10 to 90 Ohm.m, and thickness in the range from a few meters up to 12 m as shown in TDEM-AA' cross section and a few meters to 15 m in TDEM-BB' cross section.

The Electrical Resistivity Tomography (ERT) method was more efficient method than TDEM method to delineate the subsurface shallow layering and delineating the soil/bedrocks and different underground boundaries.

Acknowledgment

The authors gratefully acknowledge Al al-Bayt University- Faculty of Earth and Environmental Sciences for providing the electrical resistivity devices, and the Hashemite University - Prince El - Hasan Bin Talal Faculty of Natural Resources and Environment for providing the TDEM instrumentation. The authors appreciate very much Mr. Jafar Abu Rajab for assisting in the TDEM field surveys, and thanks to Mr. Adnan Rizq for his help during the geoelectrical field surveys.

References

Abdulla, F. and Al-Shareef, A., 2009. Roof rainwater harvesting systems for household water supply in Jordan. *Desalination,* 243 (1-3), p.195-207. DOI: 10.1016/j.desal.2008.05.013

AEMR, 2013. TEMFAST 48 HPC instrument, user guide, www.aemr.ne

AEMR, 2015. TEM-RESEARCHER Software V.8, User Guid, AEMR.

Afonso, M., Jaber, J., and Mohsen, M. 2004. Brackish groundwater treatment by reverse osmosis in Jordan. *Desalination*, 164 (2), p.157-171. DOI: 10.1016/s0011-9164(04)00175-4

Al-Amoush, H. and Mashagbeh, A., 2009. Using geophysical methods to image near-surface cylindrical pipeline: A case study on engineering applications, Jordan. *Jordan Journal of Civil Engineering*, 3 (2), p.137-149.

Al-Amoush, H., Al-Shabeeb, A.R., Al-Ayyash, S., Al-Adamat, R., Ibrahim, M., and Rajab, J.A., 2016. Geophysical and hydrological investigations of the Northern Wadis Area of Azraq Basin for groundwater artificial recharge purposes. *International Journal of Geoscience,* 7 (5), p.744-760. DOI: 10.4236/ijg.2016.75057

Al-Amoush, H, and Abu Rajab, J. 2018. The Use of Electrical Resistivity Tomography to Investigate Basaltic Lava Tunnel Based on the Case Study of Al-Badia Cave in Jordan. *Indonesian Journal on Geosciences*, 5 (2), p.161-177. DOI: 10.17014/ijog.5.2.161-177

Al-Amoush, H., Rajab, J., and Al-Tarazi, E., 2017. Electrical resistivity tomography modeling of vertical lithological contact using different electrode configurations. *Jordan Journal of Earth and Environmental Sciences*, 8 (1), p.27-34.

Al-Heety, A. and Shanshal, Z., 2016. Integration of seismic refraction tomography and electrical resistivity tomography in engineering geophysics for soil characterization. *Arabian Journal of Geosciences*, 9 (1), p.73-84. DOI: 10.1007/s12517-015-2116-9

Al-Kloub, B. and Al-Shemmeri, A., 1995. Sustainable development of water resources and possible enhancement technologies and application of water supply in Jordan. *Water International*, 20 (2), p.106-109. DOI: 10.1080/02508069508686458

Al-Momani, I., 2008. Wet and dry deposition fluxes of inorganic chemical species at a rural site in Northern Jordan. *Archives of Environmental Contamination and Toxicology*, 55 (4), p.558-565. DOI: 10.1007/s00244-008-9148-z

Baban, S. and Al-Ansari, N., 2001. Living with water scarsity-Water resources in the Jordan Badia region-The way forward. *Publication of Al al-Bayt University*, Al Mafraq, 208pp. DOI: 10.14525/jjce.10.3.3609

Barsukov O., Fainberg B., and Khabensky O., 2007. Shallow inves-tigation by TEM-FAST technique: methodology and case histories. *Methods of Geochemistry and Geophysics*, 40, p.55-77. DOI: 10.1016/s0076-6895(06)40003-2

Barrocu, G. and Ranieri, G., 2000. TDEM: A useful tool for identifying and monitoring the fresh-saltwater interface. *In*: 16th Salt Water Intrusion Meeting, Międzyzdroje, Poland, 12 (15), p.1-7.

Bauer-Gottwein, P., Gondwe, B., Christiansen, L., Herckenrath, D., Kgotlhang, L., and Zimmermann, S., 2010. Hydrogeophysical exploration of three-dimensional salinity anomalies with the time-domain electromagnetic method (TDEM). *Journal of Hydrol-*

ogy, 380 (3-4), p.318-329. DOI: 10.1016/j.jhydrol.2009.11.007

Benson, K., Payne, L., and Stubben, A., 1997. Mapping groundwater contamination using dc resistivity and VLF geophysical methods; a case study. *Geophysics*, 62 (1), p.80-86. DOI: 10.1190/1.1444148

Christiansen, A., Auken, E., and Sørensen, K., 2006. The transient electromag-netic method. *Groundwater geophysics*, p.179-225. DOI: 10.1007/3-540-29387-6_6

Colombo, D., Keho, T., and McNeice, G., 2012. Integrated seismic-electro-magnetic workflow for subbasalt exploration in northwest Saudi Arabia. *The Leading Edge*, 31 (1), p.42-52. DOI: 10.1190/1.3679327

Danielsen, J., Auken, E., Jørgensen, F., Søndergaard, V., and Sørensen, K.I., 2003. The application of the transient electromagnetic method in hydrogeophysical surveys. *Journal of Applied Geophysics*, 53 (4), p.181-198. DOI: 10.1016/j.jappgeo.2003.08.004

Dawson, C., Lane, J., White, E., and Belaval, M., 2002. Integrated geophysical characterization of the Winthrop landfill southern flow path, Winthrop, Maine. *In*: *15th EEGS Symposium on the Application of Geophysics to Engineering and Environmental Problems* (p. cp-191). DOI: 10.3997/2214-4609-pdb.191. 13esc6

de Groot-Hedlin, Constable and Steven Constable, 1990. Occam's inversion to generate smooth, two-dimensional models from magneto telluric data. *Geophysics* 55 (12), p.1613-1624. DOI: 10.1190/1.1442813

Diallo, M., Cheng, L., Rosa, E., Gunther, C., and Chouteau, M., 2019. Integrated GPR and ERT data interpretation for bedrock identification at Cléricy, Québec, Canada. *Engineering Geology*, 248, p.230-241. DOI: 10.1016/j.enggeo.2018.09.011

Farid, M., Hadi, A. I, and Sari, L. P., 2021. Investigation of Geothermal Using Magnetotelluric Method in Babakan Bogor, Bengkulu Province, Indonesia. *Indonisian Journal on Geosciences*, 8 (2), p.221-231. DOI: 10.17014/ijog.8.2.221-231.

French, R., 2011. A discussion of geophysical techniques, time domain electromagnetic exploration. Northwest geophysical associates Inc. (file: TDEM_TEQ_03.) 65pp.

Ghanem, F.K., Al Amoush, H., and Al- Tarazi, E., 2021. Geotechnical engineering evaluation of superficial deposits utilizing seismic methods at Al al-Bayt University, Jordan. *Iraqi Geological Journal*, p.11-28. DOI: 10.46717/igj.54.1d.2ms-2021-04-22

Gharaibeh, A., 2003. *Geological map of Umm Al Jimal*, *scale 1:50.000*. Natural Resources Authority. Umm Al Jimal map Sheet 3245-I.

Griffiths, D., and Barker, R., 1993. Two-dimensional resistivity imaging and modelling in areas of complex geology. *Journal of Applied Geophysics*, 29 (3-4), p.211-226. DOI: 10.1016/0926-9851(93)90005-j

Hsu, H., Yanites, B., Chen, C., and Chen, Y., 2010. Bedrock detection using 2D electrical resistivity imaging along the Peikang River, Central Taiwan. *Geomorphology*, 114 (3), p.406-414. DOI: 10.1016/j.geomorph.2009.08.004

Https://www.aabu.edu.jo/en/pages/general_information.aspx/[29 May 2020].

Jaradat, Q., Momani, K., Jiries, A., El-Alali, A., Batarseh, M., Sabri, T., and Al-Momani, I., 1999. Chemical composition of urban wet deposition in Amman, Jordan. *Water, Air, and Soil Pollution*, 112 (1-2), p.55-65. DOI: 10.1023/a:1005086616451

Loke, M., 2014. Tutorial: 2-D and 3-D electrical Imaging Surveys, Malaysia. *Geotomo Software*. 127pp.

Lowrie, W., 2007. *Fundamental of Geohysics*, 2nd edition. Cambridge University Press, 38pp.

McNeill, D., 1990. Use of electromagnetic methods for groundwater studies. *Geotechnical and Environmental Geophysics*, 1 (5), p.191-218. DOI: 10.1190/1.9781560802785.ch7

McNeill, J., 1994. Principles and application of time domain electromagnetic techniques for resistivity sounding. *Geonics Technical Note*, p.1-15.

Ministry of Water and Irrigation (MWI), 2016. National water strategy of Jordan, 2016-2025. Amman, Jordan.

Ministry of Water and Irrigation (MWI), 2018. Open file.

Nabighian, N. and Macnae, C., 1991. Time domain electromagnetic prospecting methods. *Electromagnetic methods in applied geophysics,* 2 (A), p.427-509. DOI: 10.1190/1.9781560802686.ch6

Otto, J. and Sass, O., 2006. Comparing geophysical methods for talus slope investigations in the Turtmann valley (Swiss Alps). *Geomorphology*, 76 (3-4), p.257-272. DOI: 10.1016/j.geomorph.2005.11.008

Porsani, J., Almeida, E., Bortolozo, C., and Santos, F., 2012. TDEM survey in an area of seismicity induced by water wells in Paraná sedimentary basin, Northern São Paulo State, Brazil. *Journal of Applied Geophysics*, 82, p.75-83. DOI: 10.1016/j.jappgeo.2012.02.005

Qdais, H. and Batayneh, F., 2002. The role of desalination in bridging the water gap in Jordan. *Desalination*, 150 (1), p.99-106. DOI: 10.1016/s0011-9164(02)00934-7

Rangel, R., Porsani, J., Bortolozo, C., and Hamada, L., 2018. Electrical resistivity tomography and TDEM applied to hydrogeological study in Taubaté basin, Brazil. *International Journal of Geosciences*, 9 (2), p.119-130. DOI: 10.4236/ijg.2018.92008

Ranieri, G., 2000. TEM Fast: A useful tool for hydrogeologists and environ-mental engineers. *Annali di Geofisica*, 43 (6), p.1147-1158.

Reynold, J., 2011. *An introduction to applied and environmental geophysics*, (2nd ed.). Wiely Blackwell, UK. 696 pp.

Reynolds, J.M., 1997. *An introduction to applied Environmental Geophysics* (England: Wiley), p.796.

Sauret, E., Beaujean, J., Nguyen, F., Wildemeersch, S., and Brouyere, S., 2015. Characterization of superficial deposits using electrical resistivity tomography (ERT) and horizontal-to-vertical spectral ratio (HVSR) geophysical methods: A case study. *Journal of Applied Geophysics*, 121, p.140-148. DOI: 10.1016/j.jappgeo.2015.07.012

Smadi, A., 1997. *Geological map of Al Mafraq, scale 1:50.000*. Natural Resources Authority. Mafraq mapsheet 3254- IV.

Thomsen, R., Søndergaard, V., and Sørensen, K., 2004. Hydrogeological mapping as a basis for establishing site-specific groundwater protection zones in Denmark. *Hydrogeology Journal*, 12 (5), p.550-562. DOI: 10.1007/s10040-004-0345-1

Wolfe, J., Richard, H., Hauser, C., and Hicks, D., 2000. Identifying potential collapse zones under highways. *In*: 13th EEGS Symposium on the Application of Geophysics to Engineering and Environmental Problems (p. cp-200). European Association of Geoscientists and Engineers. DOI: 10.3997/2214-4609-pdb.200.2000_041